

¹ Traits predict forest phenological responses to photoperiod
² more than temperature

³ Deirdre Loughnan¹, Faith A M Jones^{1, 2}, and E M Wolkovich^{1,3,4}

⁴ February 8, 2026

⁵ ¹ Department of Forest and Conservation, Faculty of Forestry, University of British Columbia, 2424
⁶ Main Mall Vancouver, BC Canada V6T 1Z4.

⁷ ² Department of Wildlife, Fish and Environmental Studies, Swedish University of Agricultural Sci-
⁸ ences, 901 83 Umeå, Sweden.

⁹ ³ Arnold Arboretum of Harvard University, 1300 Centre Street, Boston, Massachusetts, USA;

¹⁰ ⁴ Organismic & Evolutionary Biology, Harvard University, 26 Oxford Street, Cambridge, Massachusetts,
¹¹ USA;

¹² Corresponding Author: Deirdre Loughnan deirdre.loughnan@ubc.ca

¹³ Running title: Traits drive photoperiod cues in budburst

¹⁴ **Summary**

¹⁵ Shifts in the timing of spring phenology, such as budburst and leafout, can have major ecosystem
¹⁶ consequences. Understanding how species phenological responses fit within broader frameworks of
¹⁷ plant strategies may allow us to better identify these consequences and predict future impacts on
¹⁸ plant communities. Previous research suggests that species with early spring phenology exhibit a more
¹⁹ acquisitive strategy while later species appear more conservative in their growth. Yet testing these
²⁰ predictions has been slow given the high variability of spring phenology when measured in different
²¹ natural settings across space and time. Using controlled environment studies, we reduce phenological
²² variation into its component responses to chilling (cool winter temperatures), forcing (spring warming
²³ temperatures) and photoperiod, and test for trait relationships across 47 species sampled from eight
²⁴ forest communities (1428 individuals) across North America. We find phenology connects to four major
²⁵ plant functional traits—height, diameter, leaf mass per area and nitrogen content—via responses
²⁶ to photoperiod, but not temperature, but we found no relationship across two different metrics of
²⁷ wood density. Our results suggest photoperiod responses may be a critical component of how spring
²⁸ phenology fits within plant strategies, which could help predict future shifts in forest growth with
²⁹ continued climate change.

³⁰ **Introduction**

³¹ Climate change is causing species phenologies—the timing of life history events—to shift, with widespread
³² advances being observed across the tree of life (Parmesan and Yohe, 2003; Hoegh-Guldberg et al., 2018).

38 This common phenological fingerprint, however, averages over high variability across species (Thack-
39 eray et al., 2016; Cohen et al., 2018; Kharouba et al., 2018), posing a challenge to accurate forecasts.

40
41 In plants, species variation can be explained, in part, by differences in growth strategies, which are
42 generally inferred from traits (Violette et al., 2007). Decades of research on plant traits have worked
43 to build predictive models of species responses to their environment (Green et al., 2022), which could
44 explain species-level variability in phenological responses. Phenology, however, has generally been ex-
45 cluded from plant trait research due to its high inter- and intra-specific variability, making it difficult
46 to leverage existing frameworks to explain phenological variation and predict future changes. Previous
47 studies have found high variation in phenology in observational studies for the same species when
48 observed over different years or sites (Primack et al., 2009; Chuine et al., 2010). Yet variation is much
49 smaller when calculated from controlled experiments, suggesting that phenological variation can be
50 consistently decomposed into its environmental cues (e.g., temperature and photoperiod, Chuine and
51 Cour, 1999; Harrington and Gould, 2015; Flynn and Wolkovich, 2018).

52
53 Correlations between plant traits, growth strategies, and responses to environments have been synthe-
54 sized into several global frameworks, including the leaf economic spectrum (Wright et al., 2004) and
55 wood economic spectrum (Chave et al., 2009). These frameworks have identified key traits that ex-
56 hibit distinct gradients, ranging from acquisitive strategies—fast growing plants that produce cheaper
57 tissue—to conservative strategies—with plants that invest in long-lived tissue but slower growth rates
58 (Wright et al., 2004; Díaz et al., 2016). In temperate systems, changes in temperature and frost risk in
59 spring can produce gradients in abiotic stress, including frost risk, soil nutrients, and light availability
60 (Sakai and Larcher, 1987; Gotelli and Graves, 1996; Augspurger, 2009), in addition to differences in
61 biotic interactions from herbivory or competition later in the season (Lopez et al., 2008; Wolkovich
62 and Ettinger, 2014). Species that vary in their timing of leafout, should therefore exhibit traits and
63 growth strategies that allow them to tolerate or avoid these abiotic and biotic factors. Leveraging in-
64 sights from predictive models of phenology with these well established trait frameworks could begin to
65 disentangle the environmental cues that shape phenology from those shaped by other trait differences
66 in plant growth strategies.

67
68 To determine whether phenology fits within major functional trait frameworks requires working across
69 within- and between-species variation. Phenological variation is generally observed in natural condi-
70 tions where the environmental cues that trigger many phenological events—primarily temperature and
71 photoperiod (Chuine, 2000; Körner and Basler, 2010)—vary across space and time, though experiments
72 can often control for this variation (Basler and Körner, 2014; Vitassee et al., 2009). Though generally
73 to a much smaller scale compared to phenology, within-species variation also occurs across other plant
74 traits (e.g., leaf and wood structure traits), including across latitudinal (Wiemann and Bruce, 2002)
75 and other environmental gradients (Pollock et al., 2012). Thus better understanding how phenology
76 and other traits correlate across species requires methods that incorporate spatial variation within
77 species.

78
79 Here, we tested whether phenological variation was aligned with existing trait frameworks using data on
80 spring budburst paired with a suite of traits that capture acquisitive to conservative growth strategies.
81 We decomposed the high phenological variation in budburst date by using experiments to estimate
82 three major phenological cues for woody plant budburst: chilling (cool winter temperatures), forcing
83 (warm spring temperatures), and photoperiod. We predicted that early spring species, which generally
84 budburst before canopy closure due to smaller responses to temperature and photoperiod, would have
85 traits associated with acquisitive growth. They would thus be shorter, with smaller trunks or stem
86 diameters, and a lower investment in wood structure and leaf tissue, resulting in low wood specific
87 density, diffuse-porous wood anatomy, and low leaf mass per area, but high leaf nitrogen content for a
88 greater photosynthetic potential. In contrast, we predict species with later budburst to predominately
89 include canopy species that express more conservative growth strategies and require more chilling,

90 warmer forcing, and longer photoperiods. These species should incur greater investments in long-lived
91 tissue, with ring-porous wood anatomy, taller heights and greater diameter, denser wood and high leaf
92 mass per area, but low leaf nitrogen content. We then used a joint-modeling approach to estimate
93 the relationships between these plant traits and phenological responses to cues, while partitioning the
94 variance from species- and population-level differences.

95 Materials and Methods

96 Field sampling

97 We combined *in situ* trait data with budburst data from two growth chamber cutting experiments
98 conducted across eastern and western temperate deciduous forests in North America. We collected
99 both suites of data from populations that span a latitudinal gradient of 4-6° for the eastern and
100 western communities respectively. We took trait measurements from across eight populations, of
101 which there were four eastern populations—Harvard Forest, Massachusetts, USA (42.55°N, 72.20°W),
102 White Mountains, New Hampshire, USA (44.11°N, 52.14°W), Second College Grant, New Hampshire,
103 USA (44.79°N, 50.66°W), and St. Hippolyte, Quebec, Canada (45.98°N, 74.01°W), and four western
104 population—E.C. Manning Park (49.06°N, 120.78°W), Sun Peaks (50.88°N, 119.89°W), Alex Fraser
105 Research Forest (52.14°N, 122.14°W), and Smithers (54.78°N, 127.17°W), British Columbia (BC),
106 Canada (Fig. 1). For the two growth chamber studies on budburst phenology, we collected cuttings
107 from the most southern and northern populations in each transect ($n_{pop}=4$).
108

109 Functional traits

110 We measured all traits in the summer prior to each growth chamber study (eastern transect: 8-25 June
111 2015, western transect: 29 May to 30 July 2019), following full leafout but before budset. At each
112 population and for each species, we measured a total of five traits from 1-10 healthy adult individuals:
113 height, diameter of the main trunk or stem (hereafter referred to as diameter), wood specific density,
114 leaf mass per area, and the percent leaf nitrogen content. We also obtained xylem structure data from
115 the WSL xylem database (Schweingruber and Landolt, 2010) for 72.3% of our species.
116

117 We measured traits in accordance to the methods discussed by Pérez-Harguindeguy et al. (2013).
118 We calculated tree height using trigonometric methods and used a base height of 1.37 m to measure
119 diameter (Magarik et al., 2020). For shrub heights, we measured the distance from the ground to the
120 height of the top foliage and measured stem diameters at approximately 1 cm above ground-level. All
121 stem and leaf samples were kept cool during transport and measurements of leaf area and stem volume
122 taken within 3 and 12 hours of sample collection respectively. To measure wood specific density, we
123 collected a 10 cm sample of branch wood, taken close to the base of the branch at the stem and
124 calculated stem volume using the water displacement method. For our leaf traits, we haphazardly
125 selected and sampled five, fully expanded, and hardened leaves, with no to minimal herbivore damage.
126 We took a high resolution scan of each leaf using a flatbed scanner and estimated leaf area using the
127 ImageJ software (version 2.0.0).

128 Growth chamber study

129 For our growth chamber studies, we collected dormant branch cuttings from our highest and lowest
130 latitude populations in each transect, with sampling in our eastern study occurring from 20-28 Jan-
131 uary 2015 and sampling for our western study from 19-28 October 2019. Dormant branch cuttings
132 have been repeatedly shown to approximate whole plant responses in budburst (Vitasse and Basler,
133 2014), allowing us to estimate responses to environmental cues. In both studies, we included a total
134 of eight distinct treatments consisting of two levels of chilling, forcing, and photoperiods (Fig. 1). We

135 recorded budburst stages of each sample every 1-3 days for up to four months, defining the day of
 136 budburst as the day of budbreak or shoot elongation (denoted as code 07 by Finn et al. (2007)). For
 137 a more detailed discussion of study sample collection and methods see (Flynn and Wolkovich, 2018)
 138 for details on our eastern study and Loughnan and Wolkovich (in prep) for details on our western study.
 139

140 Statistical Analysis

141 We combined our *in situ* trait data with budburst data from the controlled environment experiments
 142 through a joint Bayesian model for each trait. This approach improves upon previous analyses of mul-
 143 tiple traits, as it allows us to carry through uncertainty between trait and phenology estimates—and
 144 better partitions the drivers of variation in species phenologies.

145 Our joint model consists of two parts. The first is a hierarchical linear model, which partitions the vari-
 146 ation of individual observations (i) of a given trait value (Y_{trait}) to account for the effects of species
 147 (j), population-level differences arising from transects, latitude, as well as the interaction between
 148 transects and latitude ($\text{transect} \cdot \text{latitude}$), and finally, residual variation or ‘measurement error’ (σ_m^2).
 149

$$Y_{\text{trait}_{i,j}} \sim \text{Normal}(\mu_{i,j}, \sigma_m^2) \quad (1)$$

$$\mu_{i,j} = \alpha_{\text{grand trait}} + \alpha_{\text{trait}_j} + \beta_{\text{transect}} \times \text{transect} + \quad (2)$$

$$\beta_{\text{latitude}} \times \text{latitude} + \beta_{\text{transect} \cdot \text{latitude}} \times (\text{transect} \cdot \text{latitude}) \quad (3)$$

$$(4)$$

151

$$\boldsymbol{\alpha}_{\text{trait}} \begin{bmatrix} \alpha_{\text{trait}_1} \\ \alpha_{\text{trait}_2} \\ \dots \\ \alpha_{\text{trait}_n} \end{bmatrix} \text{ such that } \boldsymbol{\alpha}_{\text{trait}} \sim \text{Normal}(0, \sigma_{\text{trait}}^2) \quad (5)$$

$$(6)$$

152 We included transect as a dummy variable (0/1) and latitude as a continuous variable and modeled
 153 traits in their original units, with the exception of leaf mass per area which was rescaled by 100 and
 154 wood specific density which was rescaled by 10 for numeric stability. Our model also included partial
 155 pooling for species—which controls for uneven sampling and trait variability. These species-level esti-
 156 mates are then predictors for each cue ($\beta_{\text{chilling},j}$, $\beta_{\text{forcing},j}$, $\beta_{\text{photoperiod},j}$).
 157

$$\beta_{\text{chilling}_j} = \alpha_{\text{chilling},j} + \beta_{\text{trait.chilling}} \times \alpha_{\text{trait},j} \quad (7)$$

$$\beta_{\text{forcing}_j} = \alpha_{\text{forcing},j} + \beta_{\text{trait.forcing}} \times \alpha_{\text{trait},j}$$

$$\beta_{\text{photoperiod}_j} = \alpha_{\text{photoperiod},j} + \beta_{\text{trait.photoperiod}} \times \alpha_{\text{trait},j}$$

158 In addition to the species-level estimates, this part of our model estimates the overall effect of each
 159 trait on each cue ($\beta_{\text{trait.chilling}}$, $\beta_{\text{trait.forcing}}$, $\beta_{\text{trait.photoperiod}}$). From this we could estimate how well
 160 traits explain species-level differences—by estimating the the species-level cue variation not explained
 161 by traits ($\alpha_{\text{chilling},j}$, $\alpha_{\text{forcing},j}$, $\alpha_{\text{photoperiod},j}$) and individual species responses to cues (*chilling*, *forcing*,
 162 *photoperiod*, respectively). Finally, our model estimates the residual budburst variation across species

163 $(\alpha_{\text{pheno},j})$, observations (σ_d^2), as well as the variation in cues not attributed to the trait (using partial
 164 pooling).

$$Y_{\text{pheno}_{i,j}} \sim \text{Normal}(\mu_{i,j}, \sigma_d^2) \quad (8)$$

165 with

$$\mu_{i,j} = \alpha_{\text{pheno}_j} + \beta_{\text{chilling}_j} \cdot \text{chilling} + \beta_{\text{forcing}_j} \cdot \text{forcing} + \beta_{\text{photoperiod}_j} \cdot \text{photoperiod} \quad (9)$$

166 where α_{pheno_j} , $\alpha_{\text{chilling}_j}$, $\alpha_{\text{forcing}_j}$, and $\alpha_{\text{photoperiod}_j}$ are elements of the normal random vectors:

$$\boldsymbol{\alpha}_{\text{pheno}} = \begin{bmatrix} \alpha_{\text{pheno}_1} \\ \alpha_{\text{pheno}_2} \\ \dots \\ \alpha_{\text{pheno}_n} \end{bmatrix} \text{ such that } \boldsymbol{\alpha}_{\text{pheno}} \sim \text{Normal}(\mu_{\text{pheno}}, \sigma_{\text{pheno}}^2) \quad (10)$$

$$\boldsymbol{\alpha}_{\text{chilling}} = \begin{bmatrix} \alpha_{\text{chilling}_1} \\ \alpha_{\text{chilling}_2} \\ \dots \\ \alpha_{\text{chilling}_n} \end{bmatrix} \text{ such that } \boldsymbol{\alpha}_{\text{chilling}} \sim \text{Normal}(\mu_{\text{chilling}}, \sigma_{\text{chilling}}^2) \quad (11)$$

$$\boldsymbol{\alpha}_{\text{forcing}} = \begin{bmatrix} \alpha_{\text{forcing}_1} \\ \alpha_{\text{forcing}_2} \\ \dots \\ \alpha_{\text{forcing}_n} \end{bmatrix} \text{ such that } \boldsymbol{\alpha}_{\text{forcing}} \sim \text{Normal}(\mu_{\text{forcing}}, \sigma_{\text{forcing}}^2) \quad (12)$$

$$\boldsymbol{\alpha}_{\text{photoperiod}} = \begin{bmatrix} \alpha_{\text{photoperiod}_1} \\ \alpha_{\text{photoperiod}_2} \\ \dots \\ \alpha_{\text{photoperiod}_n} \end{bmatrix} \text{ such that } \boldsymbol{\alpha}_{\text{photoperiod}} \sim \text{Normal}(\mu_{\text{photoperiod}}, \sigma_{\text{photoperiod}}^2) \quad (13)$$

(14)

167 We modeled each trait individually, with the exception of ring-porosity, which we compared across
 168 species using the posterior estimates of our wood stem density model, allowing us to account for inher-
 169 ent differences in wood anatomy across species and growth form. We included all three cues (chilling,
 170 forcing, and photoperiod) as continuous variables in our model, as well as all two-way interactions
 171 between cues and between cues and sites. We converted chilling temperatures to total chill portions,
 172 including both the chilling experienced in the field prior to sampling and during the experiment. For
 173 this we used local weather station data and the chillR package (v. 0.73.1, Luedeling, 2020). To account
 174 for differences in thermoperiodicity between the two studies (Buonaiuto et al., 2023), we also converted
 175 forcing temperatures to mean daily temperatures for each treatment. Finally, we *z*-scored each cue
 176 and site using two standard deviations to allow direct comparisons between results across parameters
 177 (Gelman, 2008).

178

179 We used trait-specific priors that were weakly informative. We validated our choice of priors using
 180 prior predictive checks and confirmed model stability under wider priors. All models were coded
 181 in the Stan programming language for Bayesian models using the rstan package (Stan Development
 182 Team, 2018) in R version 4.3.1 (R Development Core Team, 2017). All models met basic diagnostic
 183 checks, including no divergences, high effective sample sizes (n_{eff}) that exceeded 10% of the number of
 184 iterations, and \hat{R} values close to 1. We report our model estimates as the mean values with 90% uncer-
 185 tainty intervals (UI), interpreting parameter estimates with intervals that include zero to have no effect.

186

187 **Results**

188 Across our eight populations, we measured 47 unique species of which 28 were in our eastern transect
189 and 22 in our western transect. These include species dominant in both the understory and canopy
190 layer, with our eastern community consisting of 13 shrubs and 15 trees, our western community con-
191 sisting of 18 shrubs and 4 trees, and three species that occurred in both transects. In total we measured
192 traits of 1428 unique individuals between the two transects across our five *in situ* traits: height ($n =$
193 1317), diameter ($n = 1220$), wood stem density ($n = 1359$), leaf mass per area ($n = 1345$), leaf nitrogen
194 content ($n = 1351$). Across our two growth chamber studies, we made observations of 4211 branch
195 cuttings, with our observations of budburst spanning 82 and 113 days for our eastern and western
196 studies respectfully.

197 Most of our traits showed some variation by latitude within each transect, with a strong interactive
198 effect between transect and latitude (Fig. 2). Leaf nitrogen content was the only trait to vary with
199 latitude alone, with low latitude communities on both our eastern and western transects having greater
200 values of leaf nitrogen content than communities at higher latitudes (-0.1 percent per degree latitude,
201 UI: -0.2, 0.0, Table S6). Plant diameter increased with increasing (higher) latitudes in both eastern
202 and western communities (0.5 cm per degree latitude, UI: 0.1, 0.9), with a larger effect in eastern com-
203 munities (Fig. 2d). Relationships with height, woody stem density and leaf mass per area were more
204 complex. Heights and wood stem density increased with increasing latitude in western communities,
205 but decreased with latitude in eastern communities (-0.2 m per degree latitude, UI: -0.4, 0.0 for our
206 height model and -0.01 g/cm³ per degree latitude, UI: -0.02, 0.0 for our wood stem density model;
207 Fig. 2 a and c), while for leaf mass per area we found the reverse (decreasing leaf mass per area with
208 increasing latitudes in western communities, while increasing with latitude in eastern communities
209 (0.005 g/cm² per degree latitude, UI: 0.004, 0.006; Fig. 2d). In addition to the differences we found
210 across populations, we also observed large differences between individual species, which varied up to 7
211 fold for some traits (Fig. 3).

212 We found that three of our four traits had a strong relationship with photoperiod, but not always in
213 the direction we predicted. Taller species with larger trunk diameters and leaves with high nitrogen
214 content had larger responses with longer photoperiods (Fig. 3 c, i, o; Tables S2, S3, S6). But, con-
215 trary to our expectation, species with denser, high leaf mass per area leaves had smaller photoperiod
216 responses, allowing them to potentially budburst under shorter photoperiods (Fig. 3f).

217 Temperature cues ($\beta_{\text{trait.chilling}}$ and $\beta_{\text{trait.forcing}}$) exhibited no relationships with individual traits, but
218 by accounting for the effects of leaf or wood traits, we found the individual importance of our three
219 cues on budburst to vary by trait. Of the three cues, chilling (β_{chilling}) was the strongest in our models
220 of height (-13.4 days per standardized chill portions, UI: -17.2, -9.9), diameter (-12.5 days per stan-
221 dardized chill portions, UI: -16.2, -8.6), wood stem density (-2.1 days per standardized chill portions,
222 UI: -3.3, -9.8), and leaf nitrogen content (-35.1 days per standardized chill portions, UI: -68.1, -4.1),
223 with more chilling advancing budburst. Our model of leaf mass per area, however, estimated photope-
224 riod as the strongest cue ($\beta_{\text{photoperiod}}$, -14.0 days per standardized photoperiod, UI: -23.1, -3.5). After
225 accounting for the effects of traits, only our height and diameter model found all three environmental
226 cues to drive budburst timing (Tables S2, S3). Our models of wood stem density and leaf nitrogen
227 content in turn found temperature cues alone to shape budburst (Tables S4, S6), while our model of
228 leaf mass per area found a large response to only photoperiod (Table S5).

229 We found that only some of our trait models estimated clear gradients in species timing between trees
230 and shrubs, as is commonly expected. In particular, we found height had large correlations between
231 budburst timing and trait values, with earlier estimates of budburst for shrubs (with a mean day of
232 budburst of 10)—especially under greater cues—and later budburst estimates for trees (with a mean
233 day of budburst of 17.3, Fig. S1). But this was not the case for the leaf traits. Leaf nitrogen content,

238 in particular, showed no distinct separation between shrub and tree functional groups (Fig. S1).

239

240 Discussion

241 Using a joint modeling approach to understand how phenology may fit within acquisitive to conservative
242 plant strategies, we found that photoperiod related to our suite of leaf and wood traits. While budburst
243 responses to photoperiod are often much smaller than temperature responses (chilling and forcing
244 Laube et al., 2014; Zohner et al., 2016; Flynn and Wolkovich, 2018), our results suggest photoperiod
245 may be the most important cue in linking spring phenology to functional traits. Our results suggest
246 that fully predicting these responses also requires considering variation across space given differences
247 between our eastern and western transects and with latitude. These spatial differences in trait variation
248 may be due to differences in the community assemblages, as our western community was more shrub
249 dominated, with shorter plants with less dense branch wood, suggesting a more acquisitive growth
250 strategy to allow species to utilize resources early in the season before canopy closure.

251 Cues and functional traits

252 We found only partial support for our prediction that species with acquisitive traits—particularly small
253 trees with low wood density, low leaf mass per area, and high leaf nitrogen content—would have smaller
254 temperature and photoperiod responses (associated with early budburst). Species with smaller heights
255 and diameters did have smaller photoperiod responses, but—contrary to our prediction—species with
256 less dense leaves showed larger responses to photoperiod, while leaves with high nitrogen content had
257 stronger photoperiod responses. None of our focal traits, however, showed a relationship with temper-
258 ature (chilling or forcing), which may be due to selection on other physiological processes. Many of
259 our traits are associated with one or more ecological function (Wright et al., 2004; Pérez-Harguindeguy
260 et al., 2013; Reich, 2014). In particular, leaf mass per area is known to correlate with traits like leaf
261 lifespan or decomposition rates in addition to light capture (De La Riva et al., 2016). While our
262 results highlight the ways in which phenology partially aligns with gradients found in established trait
263 frameworks, they also offer new insight into potential tradeoffs in how varying physiological processes
264 shape species growth strategies.

265

266 Decades of previous phenology research have found budburst timing to be primarily driven by temper-
267 ature (chilling and forcing) and weakly by photoperiod (Chuine et al., 2010; Basler and Körner, 2014;
268 Laube et al., 2014). Yet we found no traits that correlated with responses to temperature, suggesting
269 other drivers may impact leaf and structural traits in temperate forests. One potential abiotic driver
270 we did not consider is soil moisture, which covaries with a number of traits, including leaf mass per
271 area, as higher leaf area allows plants to reduce evaporation under dry conditions (De La Riva et al.,
272 2016). Soil moisture also shapes other phenological events in woody plants, including radial growth
273 phenology and shoot elongation (Cabon et al., 2020; Peters et al., 2021). Though temperate forests are
274 generally moist compared to other systems, previous studies suggests soil moisture can shape spring
275 phenology across xeric systems as well (Crimmins et al., 2011; Park, 2014; Ettinger et al., 2019), thus
276 including it in future studies could help understand how species growth strategies correlate with phe-
277 nology.

278

279 Our finding that budburst was not related to wood structure or wood stem density contrasts the
280 findings of previous work linking these traits. Previous studies have found some evidence that trees
281 with diffuse-porous wood structure leafout earlier than species with ring-porous structures (Lechowicz,
282 1984; Panchen et al., 2014; Yin et al., 2016; Osada, 2017; Savage et al., 2022). Using wood density
283 as an alternative measure of wood structure (wood density positively correlates with xylem resistance
284 to embolism, Hacke et al., 2001), we did not find an association between our three phenological cues

and xylem structure, despite our data including similar temperate forest species to previous studies. This could be because we captured additional variation by sampling many individuals for each species across a large spatial gradient. In particular, we found larger wood densities at higher latitudes in our western transect, which could be caused by the differences in winter conditions experienced across this transect. Higher wood densities are especially favorable in communities that experience greater horizontal stress from wind and downward pressure from snow (MacFarlane and Kane, 2017; MacFarlane, 2020). Relationships with wood density may also be more apparent over a larger span of wood specific densities (our values varied from 0.2 to 0.6 g/cm³, which is smaller than seen in studies that span a more global distribution Galvão et al., 2021; Savage et al., 2022; Mo et al., 2024).

In addition to our study providing insight into how trait-budburst relationships vary with latitude, our sites also spanned North America, encompassing a gradient of 55° in longitude. At this continental scale we found correlations between phenology and traits for woody species in temperate forests, but these may shift with data that expands across biomes and more plant functional groups. Indeed, both the leaf and wood economic spectra find that large variation in traits across species, which arises from large global datasets that include both temperate and tropical species (Wright et al., 2004; Díaz et al., 2016; Chave et al., 2009) and functional groups that span from trees to grasses (Wright et al., 2004). Global patterns in trait variation may also be absent at smaller spatial scales (Wright and Sutton-Grier, 2012; Messier et al., 2017a,b), suggesting that comparisons of trait-phenology relationships at larger spatial scales or across more diverse pools of species may better align with the patterns predicted by existing economic spectra.

In comparing our results with a global meta-analysis of tree trait relationships with budburst cues (Loughnan et al., 2025), we however found similar trait-cue relationships for two traits: height and leaf mass per area. At both the global and continental scales, trees with taller heights leafed out with longer photoperiods. We also found species with high specific leaf area—which is the inverse of leaf mass per area and thus equivalent to low values—exhibited large responses to photoperiod (Loughnan et al., 2025). The consistency of these results, despite the differences in the two spatial scales of these datasets, provides further support that woody species responses to photoperiod may be part of a larger plant strategy.

315

316 Functional traits predict climate change responses

317 Our results offer novel insights into how broader correlations between growth strategies and phenological cues can help predict responses in woody plant communities with climate change. As temperatures rise, particularly at higher latitudes (Hoegh-Guldberg et al., 2018), warmer winter and spring temperatures may select for earlier budburst in some species. But, since photoperiod will remain fixed, our 318 observed relationships between photoperiod and other traits has the potential to limit species abilities 319 to track temperatures. This could constrain the extent to which some species growth will advance with 320 climate change. Our results suggest that these effects will likely be greater for taller species or canopy 321 trees and species with relatively low leaf mass per area. These constraints could have cascading effects 322 on forest communities, as variable species responses to increasing temperatures further alter species 323 growth strategies and their interactions with competitors or herbivores within their communities.

327

328 Our findings of correlations between phenology and other commonly measured traits highlight how 329 accurate forecasts of future changes in phenology could benefit from accounting for the response of 330 other traits to climate change. Across temperature and precipitation gradients, leaf size and shape 331 also change, as species shift to conserve water and mitigate effects of transpiration under higher tem- 332 peratures (De La Riva et al., 2016). These changes could impact species photosynthetic potential and 333 ultimately ecosystem services, such as carbon sequestration. While phenological research has focused 334 on forecasting responses to temperature, the correlation of other traits with photoperiod suggests it is

335 also an important cue. By considering the tradeoffs and differences in cues that simultaneously shape
336 plants growth strategies, we can more accurately forecast species phenology and community dynamics
337 under future climates.

338

339 References

- 340 Augspurger, C. K. 2009. Spring 2007 warmth and frost: phenology, damage and refoliation in a
341 temperate deciduous forest. *Functional Ecology* 23:1031–1039.
- 342 Basler, D., and C. Körner. 2014. Photoperiod and temperature responses of bud swelling and bud
343 burst in four temperate forest tree species. *Tree Physiology* 34:377–388.
- 344 Buonaiuto, D. M., E. M. Wolkovich, and M. J. Donahue. 2023. Experimental designs for testing the
345 interactive effects of temperature and light in ecology : The problem of periodicity. *Functional
346 Ecology* 37:1747–1756.
- 347 Cabon, A., L. Fernández-de-Uña, G. Gea-Izquierdo, F. C. Meinzer, D. R. Woodruff, J. Martínez-
348 Vilalta, and M. De Cáceres. 2020. Water potential control of turgor-driven tracheid enlargement in
349 Scots pine at its xeric distribution edge. *New Phytologist* 225:209–221.
- 350 Chave, J., D. Coomes, S. Jansen, S. L. Lewis, N. G. Swenson, and A. E. Zanne. 2009. Towards a
351 worldwide wood economics spectrum. *Ecology Letters* 12:351–366.
- 352 Chuine, I. 2000. A unified model for budburst of trees. *Journal of Theoretical Biology* 207:337–347.
- 353 Chuine, I., and P. Cour. 1999. Climatic determinants of budburst seasonality in four temperate-zone
354 tree species. *New Phytologist* 143:339–349.
- 355 Chuine, I., X. Morin, and H. Bugmann. 2010. Warming, photoperiods, and tree phenology. *Science*
356 329:277–278.
- 357 Cohen, J. M., M. J. Lajeunesse, and J. R. Rohr. 2018. A global synthesis of animal phenological
358 responses to climate change. *Nature Climate Change* 8:224–228.
- 359 Crimmins, T. M., M. A. Crimmins, and C. D. Bertelsen. 2011. Onset of summer flowering in a ‘Sky
360 Island’ is driven by monsoon moisture. *New Phytologist* 191:468–479.
- 361 De La Riva, E. G., M. Olmo, H. Poorter, J. L. Ubera, and R. Villar. 2016. Leaf Mass per Area (LMA)
362 and Its Relationship with Leaf Structure and Anatomy in 34 Mediterranean Woody Species along a
363 Water Availability Gradient. *PLOS ONE* 11:e0148788.
- 364 Díaz, S., J. Kattge, J. H. Cornelissen, I. J. Wright, S. Lavorel, S. Dray, B. Reu, M. Kleyer, C. Wirth,
365 I. Colin Prentice, E. Garnier, G. Bönisch, M. Westoby, H. Poorter, P. B. Reich, A. T. Moles, J. Dickie,
366 A. N. Gillison, A. E. Zanne, J. Chave, S. Joseph Wright, S. N. Sheremet Ev, H. Jactel, C. Baraloto,
367 B. Cerabolini, S. Pierce, B. Shipley, D. Kirkup, F. Casanoves, J. S. Joswig, A. Günther, V. Falcuk,
368 N. Rüger, M. D. Mahecha, and L. D. Gorné. 2016. The global spectrum of plant form and function.
369 *Nature* 529:167–171.
- 370 Ettinger, A. K., I. Chuine, B. I. Cook, J. S. Dukes, A. M. Ellison, M. R. Johnston, A. M. Panetta,
371 C. R. Rollinson, Y. Vitassee, and E. M. Wolkovich. 2019. How do climate change experiments alter
372 plot-scale climate? *Ecology Letters* 22:748–763.
- 373 Finn, G. A., A. E. Straszewski, and V. Peterson. 2007. A general growth stage key for describing trees
374 and woody plants. *Annals of Applied Biology* 151:127–131.

- 375 Flynn, D. F. B., and E. M. Wolkovich. 2018. Temperature and photoperiod drive spring phenology
376 across all species in a temperate forest community. *New Phytologist* 219:1353–1362.
- 377 Galvão, F. G., A. L. Alves De Lima, C. Candeia De Oliveira, V. F. Da Silva, and M. J. N. Rodal.
378 2021. The importance of wood density in determining the phenology of tree species in a coastal rain
379 forest. *Biotropica* 53:1134–1141.
- 380 Gelman, A. 2008. Scaling regression inputs by dividing by two standard deviations. *Statistics in
381 Medicine* 27:2865–2873.
- 382 Gotelli, N. J., and G. R. Graves. 1996. The temporal niche. Pages 95–112 in *Null Models In Ecology*.
383 Smithsonian Institution Press, Washington, D. C.
- 384 Green, S. J., C. B. Brookson, N. A. Hardy, and L. B. Crowder. 2022. Trait-based approaches to
385 global change ecology: moving from description to prediction. *Proceedings of the Royal Society B:
386 Biological Sciences* 289:1–10.
- 387 Hacke, U. G., J. S. Sperry, W. T. Pockman, S. D. Davis, and K. A. McCulloh. 2001. Trends in wood
388 density and structure are linked to prevention of xylem implosion by negative pressure. *Oecologia*
389 126:457–461.
- 390 Harrington, C. A., and P. J. Gould. 2015. Tradeoffs between chilling and forcing in satisfying dormancy
391 requirements for Pacific Northwest tree species. *Frontiers in Plant Science* 6:1–12.
- 392 Hoegh-Guldberg, O., D. Jacob, M. Taylor, M. Bind, S. Brown, I. Camilloni, A. Diedhiou, R. Djalante,
393 K. Ebi, F. Engelbrecht, J. Guiot, Y. Hijioka, S. Mehrotra, A. Payne, S. Seneviratne, A. Thomas,
394 R. Warren, and G. Zhou. 2018. Impacts of 1.5 °C Global Warming on Natural and Human Systems.
395 In: *Global Warming of 1.5 °C. An IPCC Special Report on the impacts of global warming of 1.5 °C
396 above pre-industrial levels and related global greenhouse gas emission pathways, in the context of .
397 Tech. rep.*, Cambridge University Press, Cambridge, UK and New York, NY, USA.
- 398 Kharouba, H. M., J. Ehrlén, A. Gelman, K. Bolmgren, J. M. Allen, S. E. Travers, and E. M. Wolkovich.
399 2018. Global shifts in the phenological synchrony of species interactions over recent decades. *Pro-
400 ceedings of the National Academy of Sciences* 115:5211–5216.
- 401 Körner, C., and D. Basler. 2010. Phenology Under Global Warming. *Science* 327:1461–1463.
- 402 Laube, J., T. H. Sparks, N. Estrella, J. Höfler, D. P. Ankerst, and A. Menzel. 2014. Chilling outweighs
403 photoperiod in preventing precocious spring development. *Global Change Biology* 20:170–182.
- 404 Lechowicz, M. J. 1984. Why Do Temperate Deciduous Trees Leaf Out at Different Times? Adaptation
405 and Ecology of Forest Communities. *The American Naturalist* 124:821–842.
- 406 Lopez, O. R., K. Farris-Lopez, R. A. Montgomery, and T. J. Givnish. 2008. Leaf phenology in relation
407 to canopy closure in southern Appalachian trees. *American Journal of Botany* 95:1395–1407.
- 408 Loughnan, D., F. A. Jones, G. Legault, C. J. Chamberlain, D. M. Buonaiuto, A. K. Ettinger, M. Gar-
409 ner, D. S. Sodhi, and E. M. Wolkovich. 2025. Budburst timing within a functional trait framework.
410 *Journal of Ecology* 00:1–12.
- 411 Loughnan, D., and E. M. Wolkovich. in prep. Temporal assembly of woody plant communities shaped
412 equally by evolutionary history as by current environments .
- 413 Luedeling, E. 2020. chillR: Statistical Methods for Phenology Analysis in Temperate Fruit Trees.
414 <https://CRAN.R-project.org/package=chillR>.
- 415 MacFarlane, D. W. 2020. Functional Relationships Between Branch and Stem Wood Density for
416 Temperate Tree Species in North America. *Frontiers in Forests and Global Change* 3.

- 417 MacFarlane, D. W., and B. Kane. 2017. Neighbour effects on tree architecture: functional trade-offs
418 balancing crown competitiveness with wind resistance. *Functional Ecology* 31:1624–1636.
- 419 Magarik, Y. A., L. A. Roman, and J. G. Henning. 2020. How should we measure the dbh of multi-
420 stemmed urban trees? *Urban Forestry & Urban Greening* 47:1–11.
- 421 Messier, J., M. J. Lechowicz, B. J. McGill, C. Violette, and B. J. Enquist. 2017a. Interspecific integration
422 of trait dimensions at local scales: the plant phenotype as an integrated network. *Journal of Ecology*
423 105:1775–1790.
- 424 Messier, J., B. J. McGill, B. J. Enquist, and M. J. Lechowicz. 2017b. Trait variation and integration
425 across scales: is the leaf economic spectrum present at local scales? *Ecography* 40:685–697.
- 426 Mo, L., T. W. Crowther, D. S. Maynard, and e. a. Van Den Hoogen. 2024. The global distribution
427 and drivers of wood density and their impact on forest carbon stocks. *Nature Ecology & Evolution*
428 8:2195–2212.
- 429 Osada, N. 2017. Relationships between the timing of budburst, plant traits, and distribution of 24
430 coexisting woody species in a warm-temperate forest in Japan. *American Journal of Botany* 104:550–
431 558.
- 432 Panchen, Z. A., R. B. Primack, B. Nordt, E. R. Ellwood, A. Stevens, S. S. Renner, C. G. Willis,
433 R. Fahey, A. Whittemore, Y. Du, and C. C. Davis. 2014. Leaf out times of temperate woody
434 plants are related to phylogeny, deciduousness, growth habit and wood anatomy. *New Phytologist*
435 203:1208–1219.
- 436 Park, I. W. 2014. Impacts of differing community composition on flowering phenology throughout warm
437 temperate, cool temperate and xeric environments. *Global Ecology and Biogeography* 23:789–801.
- 438 Parmesan, C., and G. Yohe. 2003. A globally coherent fingerprint of climate change impacts across
439 natural systems. *Nature* 421:37–42.
- 440 Pérez-Harguindeguy, N., S. Díaz, E. Garnier, S. Lavorel, H. Poorter, P. Jaureguiberry, M. S. Bret-
441 Harte, W. K. Cornwell, J. M. Craine, D. E. Gurvich, C. Urcelay, E. J. Veneklaas, P. B. Reich,
442 L. Poorter, I. J. Wright, P. Ray, L. Enrico, J. G. Pausas, A. C. de Vos, N. Buchmann, G. Funes,
443 F. Quétier, J. G. Hodgson, K. Thompson, H. D. Morgan, H. ter Steege, M. G. A. van der Heijden,
444 L. Sack, B. Blonder, P. Poschlod, M. V. Vaineretti, G. Conti, A. C. Staver, S. Aquino, and J. H. C.
445 Cornelissen. 2013. New handbook for standardized measurement of plant functional traits worldwide.
446 *Australian Journal of Botany* 61:167–234.
- 447 Peters, R. L., K. Steppe, H. E. Cuny, D. J. De Pauw, D. C. Frank, M. Schaub, C. B. Rathgeber,
448 A. Cabon, and P. Fonti. 2021. Turgor – a limiting factor for radial growth in mature conifers along
449 an elevational gradient. *New Phytologist* 229:213–229.
- 450 Pollock, L. J., W. K. Morris, and P. A. Vesk. 2012. The role of functional traits in species distributions
451 revealed through a hierarchical model. *Ecography* 35:716–725.
- 452 Primack, R. B., I. Ibáñez, H. Higuchi, S. D. Lee, A. J. Miller-Rushing, A. M. Wilson, and J. A. Silan-
453 der. 2009. Spatial and interspecific variability in phenological responses to warming temperatures.
454 *Biological Conservation* 142:2569–2577.
- 455 R Development Core Team. 2017. R: A language and environment for statistical computing.
- 456 Reich, P. B. 2014. The world-wide ‘fast–slow’ plant economics spectrum: a traits manifesto. *Journal*
457 *of Ecology* 102:275–301.
- 458 Sakai, A., and W. Larcher. 1987. *Frost Survival of Plants: Responses and adaptation to freezing stress*.
459 Springer-Verlag, Berlin, Heidelberg.

- 460 Savage, J. A., T. Kiecker, N. McMann, D. Park, M. Rothendler, and K. Mosher. 2022. Leaf out time
461 correlates with wood anatomy across large geographic scales and within local communities. *New*
462 *Phytologist* 235:953–964.
- 463 Schweingruber, F., and W. Landolt. 2010. The xylem database.
- 464 Stan Development Team. 2018. RStan: the R interface to Stan. R package version 2.17.3.
- 465 Thackeray, S. J., P. A. Henrys, D. Hemming, J. R. Bell, M. S. Botham, S. Burthe, P. Helaouet,
466 D. G. Johns, I. D. Jones, D. I. Leech, E. B. MacKay, D. Massimino, S. Atkinson, P. J. Bacon,
467 T. M. Brereton, L. Carvalho, T. H. Clutton-Brock, C. Duck, M. Edwards, J. M. Elliott, S. J. Hall,
468 R. Harrington, J. W. Pearce-Higgins, T. T. Høye, L. E. Kruuk, J. M. Pemberton, T. H. Sparks,
469 P. M. Thompson, I. White, I. J. Winfield, and S. Wanless. 2016. Phenological sensitivity to climate
470 across taxa and trophic levels. *Nature* 535:241–245.
- 471 Violle, C., M. Navas, D. Vile, E. Kazakou, C. Fortunel, I. Hummel, and E. Garnier. 2007. Let the
472 concept of trait be functional! *Oikos* 116:882–892.
- 473 Vitasse, Y., and D. Basler. 2014. Is the use of cuttings a good proxy to explore phenological responses
474 of temperate forests in warming and photoperiod experiments? *Tree Physiology* 34:174–183.
- 475 Vitasse, Y., A. Josée, A. Kremer, R. Michalet, and S. Delzon. 2009. Responses of canopy duration to
476 temperature changes in four temperate tree species : relative contributions of spring and autumn
477 leaf phenology. *Oecologia* 161:187–198.
- 478 Wiemann, M. C., and W. G. Bruce. 2002. Geographic variation in wood specific gravity: effects of
479 latitude, temperature, and precipitation. *Wood and Fiber Science* 34:96–107.
- 480 Wolkovich, E. M., and A. K. Ettinger. 2014. Back to the future for plant phenology research. *New*
481 *Phytologist* 203:1021–1024.
- 482 Wright, I. J., M. Westoby, P. B. Reich, J. Oleksyn, D. D. Ackerly, Z. Baruch, F. Bongers, J. Cavender-
483 Bares, T. Chapin, J. H. C. Cornellissen, M. Diemer, J. Flexas, J. Gulias, E. Garnier, M. L. Navas,
484 C. Roumet, P. K. Groom, B. B. Lamont, K. Hikosaka, T. Lee, W. Lee, C. Lusk, J. J. Midgley,
485 Ü. Niinemets, H. Osada, H. Poorter, P. Pool, E. J. Veneklaas, L. Prior, V. I. Pyankov, S. C.
486 Thomas, M. G. Tjoelker, and R. Villar. 2004. The worldwide leaf economics spectrum. *Nature*
487 428:821–827.
- 488 Wright, J. P., and A. Sutton-Grier. 2012. Does the leaf economic spectrum hold within local species
489 pools across varying environmental conditions? *Functional Ecology* 26:1390–1398.
- 490 Yin, J., J. D. Fridley, M. S. Smith, and T. L. Bauerle. 2016. Xylem vessel traits predict the leaf
491 phenology of native and non-native understorey species of temperate deciduous forests. *Functional*
492 *Ecology* 30:206–214.
- 493 Zohner, C. M., B. M. Benito, J.-C. Svenning, and S. S. Renner. 2016. Day length unlikely to constrain
494 climate-driven shifts in leaf-out times of northern woody plants. *Nature Climate Change* 6:1120–
495 1123.

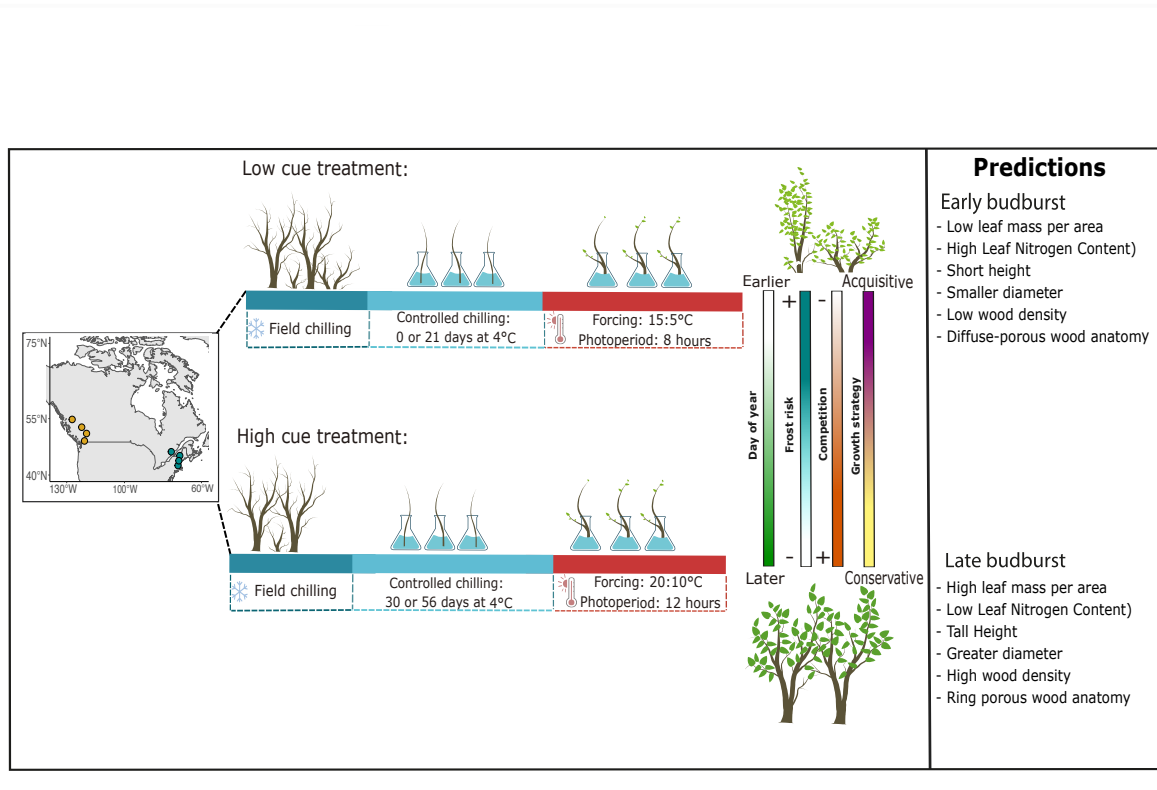


Figure 1: We collected trait data and branch cuttings from woody plants growing within eight sites, across two transects in eastern and western North America. Cuttings were used in two controlled environment studies in which we applied high and low chilling, forcing, and photoperiod treatments and recorded the day of budburst. Using our paired *in situ* trait and experimental budburst data, we tested whether earlier budbursting species exhibited traits associated with more acquisitive growth strategies and smaller responses to cues and later budbursting species a more conservative growth strategy and larger responses to cues (see ‘Predictions’ at right).

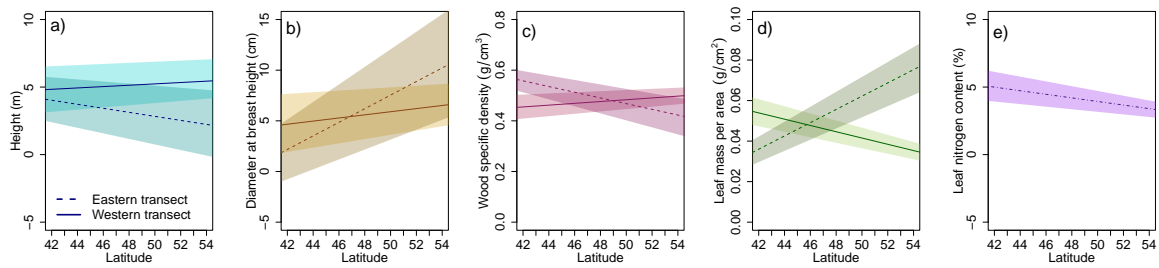


Figure 2: We found a. height, b. diameter, c. branch wood specific density, and d. leaf mass per area to all experience a strong interaction between latitude and transect, e. while leaf nitrogen content showed a strong effect of latitude alone.

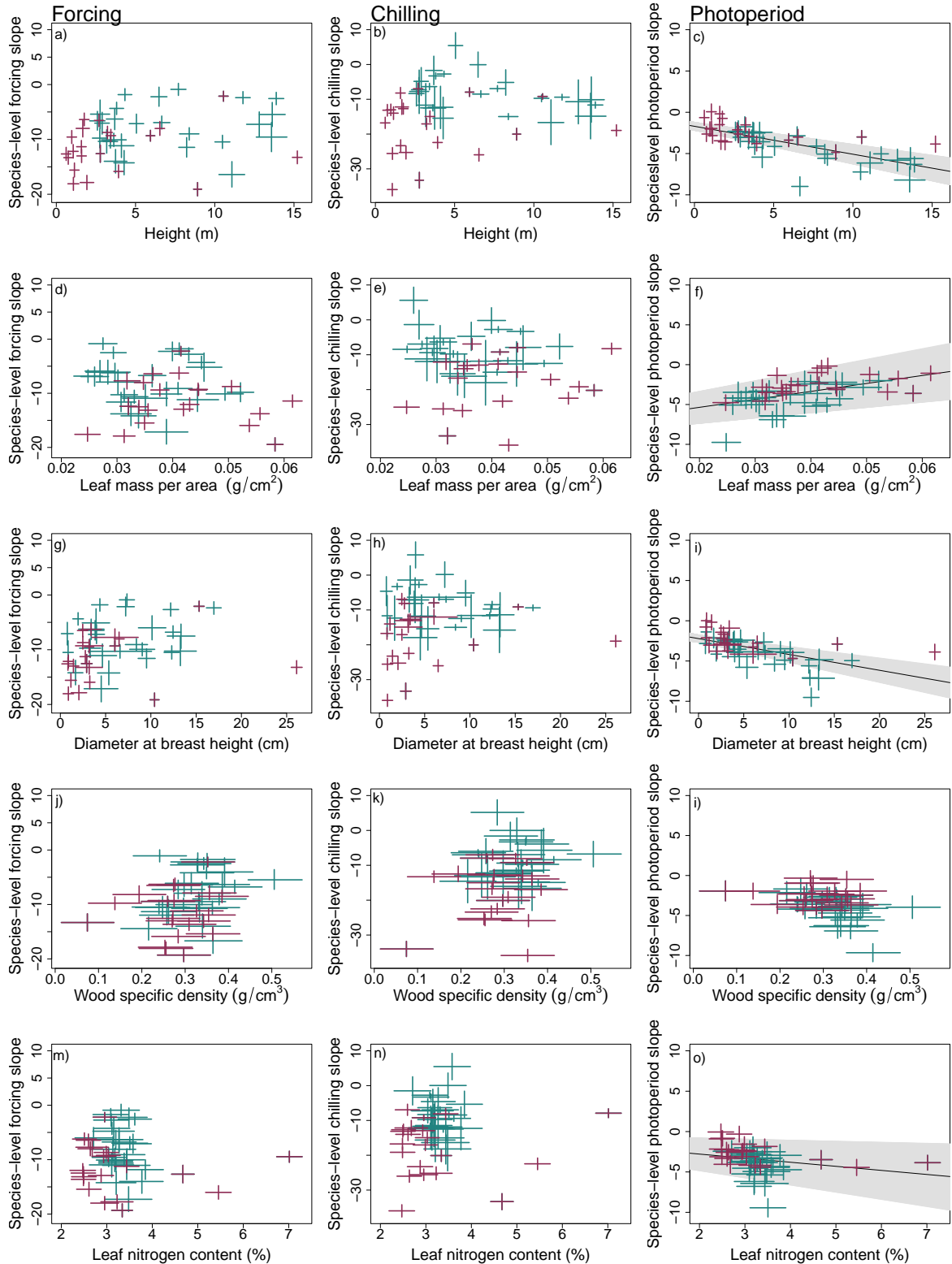


Figure 3: Relationships between species traits and cue responses showed considerable variation across a-c. height, d-f. leaf mass per area, g-i. diameter, j-l. wood specific density, and m-o. leaf nitrogen content. Point colours representing different species groups, with tree species shown in red and shrub species in blue. Crosses depict the 50% uncertainty interval of the model estimates of species trait values and estimated responses to cues. Grey bands depict large relationships between a trait and cue, representing the 90% uncertainty interval, and black lines the mean response.

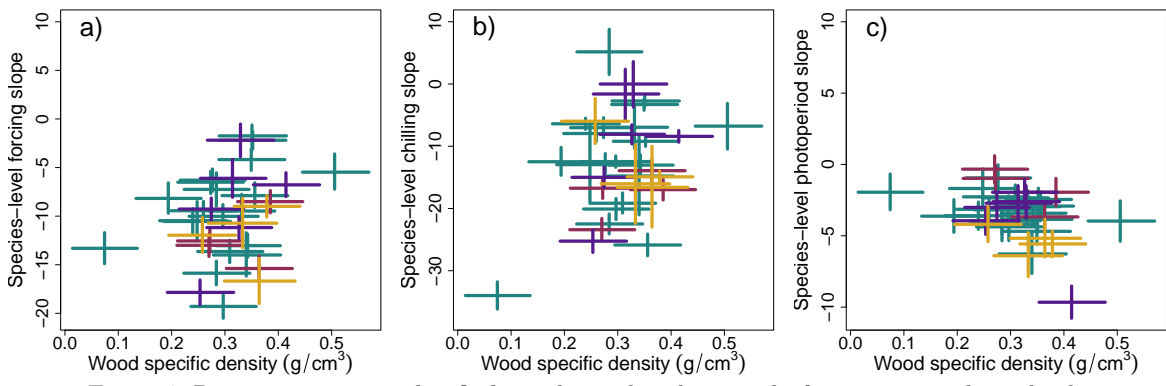


Figure 4: Despite previous studies finding relationships between leaf out timing and wood xylem structures, we did not find clear differences in species-level estimates of cue responses with wood structure or relative to their wood specific densities. Each cross represents the 50% uncertainty interval of **a.** forcing, **b.** chilling, and **c.** photoperiod responses and wood specific density for each species, with colors depicting different types of wood structure. The lowest wood specific density was estimated for *Sambucus racemosa* and the highest wood specific density for *Viburnum lantanoides*.